Local Plasticity of Al Thin Films as Revealed by X-Ray Microdiffraction

R. Spolenak* and W. L. Brown
Agere Systems, Lucent Technologies, Murray Hill, New Jersey 07974

N. Tamura, A. A. MacDowell, R. S. Celestre, and H. A. Padmore
Advanced Light Source, Berkeley, California 94720

B. Valek and J. C. Bravman
Department of Materials Science & Engineering, Stanford University, Stanford, California 94305

T. Marieb and H. Fujimoto
Intel Corporation, Santa Clara, California 95052 & Portland, Oregon 97124

B.W. Batterman and J. R. Patel
Advanced Light Source, Berkeley, California 94720, and Stanford Synchrotron Radiation Laboratories, Stanford, California 94309
(Received 12 January 2002; published 4 March 2003)

Grain-to-grain interactions dominate the plasticity of Al thin films and establish effective length scales smaller than the grain size. We have measured large strain distributions and their changes under plastic strain in 1.5-μm-thick Al 0.5% Cu films using a 0.8-μm-diameter white x-ray probe at the Advanced Light Source. Strain distributions arise not only from the distribution of grain sizes and orientation, but also from the differences in grain shape and from stress environment. Multiple active glide plane domains have been found within single grains. Large grains behave like multiple smaller grains even before a dislocation substructure can evolve.

DOI: 10.1103/PhysRevLett.90.096102 PACS numbers: 68.60.Bs, 62.20.Fe

Polycrystalline plasticity on the macroscale is strongly dependent on the behavior of single grains on the microscale as has been demonstrated by several groups experimentally [1–3] as well as theoretically [1,2,4]. In bulk polycrystalline samples inhomogeneous deformation occurs at large plastic strains due to the organization of dislocations and grain rotation. In thin films attached to single crystalline substrates, where the maximum total strain is in principal determined by the difference in CTEs (coefficients of thermal expansion), large differences in stress after cooldown from deposition temperatures are not to be expected. Macroscopic effects such as strain hardening and the so called "Bauschinger" effect [5], usually interpreted as due to a dislocation pileup at obstacles leading to an asymmetry in the yield stress in compression and tension, can be explained by phenomena on a local (grain size) scale. So far thin film models that have tried to explain those effects have failed to incorporate the grain-grain interactions on a local level. In this Letter we demonstrate that stress variations on a length scale even smaller than micron sized single grains play an important role. There are many technological implications of the mechanical properties of thin metal films, including the undesirable presence of creep in MEMS (micro-electro-mechanical systems) devices, but this Letter is confined to discussion of the new insight on plasticity provided by strain measurements with high spatial resolution.

We probe thin film Al 0.5 wt% Cu with a white x-ray beam that has been focused to less than 0.8 μm laterally [6–11]. The grain structure of the films is columnar and the third dimension of the volume accessed by the probe is given by the film thickness which is 1.5 μm. By acquiring white light Laue images at an array of different x-y positions on the sample, we are able to map the local orientation as well as the local deviatoric strain state within each grain [11–14]. Since our experiment is performed at room temperature and plasticity in this temperature range is dislocation mediated, the dilatational component of the strain tensor is of secondary importance. The dilatation can also be obtained from measurements of the energy of the Laue reflections utilizing a scanned monochromatic beam [10], but it is not included in the present measurements. The deviatoric strain tensor is converted into a deviatoric stress tensor by the application of the elastic compliance tensor [10] using literature values.

The Al(Cu) film was deposited at 400 °C on a 200-nm-thick Si-rich (compared to stoichiometric Si_3N_4) SiN_x membrane on a Si frame. This allows stresses to be applied to the metal by differential pressure bulging of the membrane. The membrane is a 2×12 mm^2 rectangle whose 1:6 aspect ratio ensures a macroscopically uniaxial stress change across the narrow dimension when the membrane is bulged. The stress state at room temperature is primarily a result of the cooldown from the 400 °C

 0031-9007/03/90(9)/096102(4)$20.00 © 2003 The American Physical Society

deposition temperature due to the difference in thermal expansion coefficients between the film and the substrate. The room temperature stress is limited by the plastic deformation of the Al-Cu film during cooldown and the stress relaxation (creep) at room temperature that has occurred over several weeks between cooldown and these measurements. By bulging, macroscopic total uniaxial strains of up to 0.2% are achieved in addition to the already-present thermal strain. This is sufficient to cause plastic deformation because the Al-Cu film is already close to its yield stress. The stress state before bulging is macroscopically biaxial. However, the stress map in the x direction (across the narrow dimension of the membrane) at room temperature, Fig. 1 [(σ'_{xx}) and (σ'_{zz})], shows that the stress state is already strongly nonbiaxial on a local scale. This observation can now be introduced into macroscopic modeling of thin films, where so far only biaxial stresses have been considered. The "ruling out" of grain boundary sliding as a mechanism responsible for anelastic processes, as could be deduced from a macroscopically biaxial stress state, is also not justified since we observe local shear stresses acting on grain boundaries, for example, at the bottom right in Fig. 1 (σ'_{xy}). In the out-of-plane stress map [Fig. 1 (σ'_{zz}) top right] one can also see negative (compressive) stress values in the deviatoric stress. At high enough values this stress state will lead to plastic deformation causing the film to shrink in plane. Upon heating which makes these stress values more negative or less positive these highly stressed areas will yield first and lead to a deviation from the expected linear thermoelastic behavior of stress versus temperature even before the film becomes macroscopically compressive. This behavior can certainly be responsible for the Bauschinger effect in thin films. Our finding of a wide distribution of stresses implies that there is a wide distribution of yield stresses. Such a strong variation in yield stresses is surprising in an elastically fairly isotropic material like aluminum.

In contrast to Cu [15], since the grain orientation [the film is weakly (111) textured] and the small elastic anisotropy of Al have only a minor influence on the yield stress, other factors must be considered. The remaining factors usually influencing the yield stress are precipitation hardening, film thickness constraint [16,17], and grain size constraint [18]. The first two factors are unlikely to be responsible for the wide distribution in yield stresses because they do not vary as a function of location in the film. Thus we concentrate on the grain size effect and introduce the concept of an "effective" grain size, which we define as the length scale over which

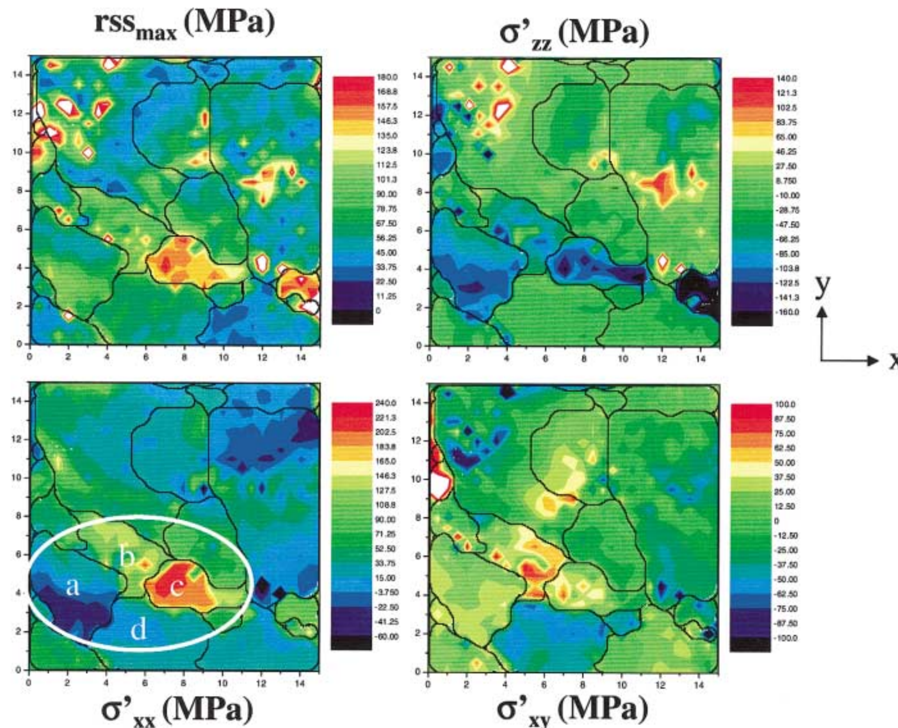

FIG. 1 (color). Deviatoric stress maps of a 15×15-μm^2 area in the center of a 1.5-μm-thick Al 0.5 wt % Cu layer on a 200-nm-thick SiN_x membrane: top left (rss_{max}): resolved shear stress on the glide system experiencing the highest shear stress, top right (σ'_{zz}): out-of-plane deviatoric stress in Z, bottom left (σ'_{xx}): in-plane deviatoric stress in X, bottom right (σ'_{xy}): in-plane deviatoric shear stress in XY; the area of interest is outlined with a white border, and grains of interest are labeled alphbetically.

dislocations are constrained. What matters in this case is not only the physical grain size, but the region within a grain over which the 3D stress state of the grain is such that the active glide system (the glide system with the highest resolved shear stress) does not change.

This can be demonstrated by looking at examples of single grains in the polycrystalline ensemble. Figure 1 shows that the stress state within one grain is strongly influenced by its neighbors. For example, in the area outlined by the white oval one sees that differences in stress within one grain are strongly correlated with grain boundaries. The stress gradient in grain a, for instance, is caused by the differences in stress in grains b and c versus grain d. Figure 2 is a simplified schematic, which illustrates a scenario that would lead to such a stress state. A force that is introduced through two grains that are connected to each other by two grains in parallel (b,c and d) which have different yield stresses will have two effects (i) a shear stress will be induced along the horizontal grain boundary (between b,c and d) and (ii) gradients in stress will arise along the vertical axis in the grains to the right and the left (e.g., grain a). The stress maps in Fig. 1 show both effects. The difference in stress between the top (b,c) and the bottom grains (d) in the area of interest causes a gradient in stress in the grain to the farthest left (grain a) [Fig. 1 (σ'_{xx}) bottom left] and a shear stress on the boundary between the two grains (b,c and d) [Fig. 1 (σ'_{xy}) bottom right].

Figure 3 shows grain a in more detail. The upper part experiences a lower maximum resolved shear stress than the lower part [vector diagram in Fig. 3(d)]. This is correlated with a change of glide systems as shown by the vector diagram. The degree of plastic deformation that this grain has experienced during cooldown can be seen by the plot of the average peak width of the diffraction spots, a measure of the defect density within the illuminated volume at each data point, as well as the orientation of the grain. In this white light measurement technique peak broadening is mostly due to line defects (giving rise to changes in orientation) rather than to strain gradients. The average peak width is higher in the upper part (where there is a lower resolved shear stress) of the grain indicating that this portion has experienced more plastic strain than the lower half. This is in agreement with the rotation of the (111) axis away from the sample normal from the top to the bottom. The change in stress coincides with the boundary between the two grains to the right (b and d) of grain a indicating that pushes and pulls from these two grains are responsible for the stress variation in grain a by a mechanism such as that shown in Fig. 2.

When the membrane is bulged and uniaxial stress is superimposed on the stress state just described the concept of an effective grain size becomes even more apparent. Figure 4 shows the evolution in maximum resolved shear stress as well as the evolution of the active glide planes as the film is brought to a uniaxial total strain of 0.2% and back. Note that as the vectors are a projection of the glide direction into the x-y plane the angle between the two glide systems is not conserved. The magnitude of the resolved shear stress does not change as the film is bulged. This grain was already at its yield stress at the beginning of the test and no local strain hardening is observed. In terms of glide systems, however, one can observe major changes. The upper part of the grain experiences a change in glide system, whereas the lower half of the grain remains unchanged. The Burger's vector is pointed to the left at high strains allowing for a deformation that elongates the film in the x direction. Hence, this grain actually behaves as two grains, rather than as one as would be anticipated from its physical size. As already mentioned this is caused by the presence of a grain boundary between the two grains on the right side (Fig. 1) of the selected grain a, with a highly stressed grain on the top (grain b) and lower stressed grain on the bottom (grain d). The magnitude of shear stresses after the plastic deformation is hardly changed in comparison to the original state as the plastic strain was small.

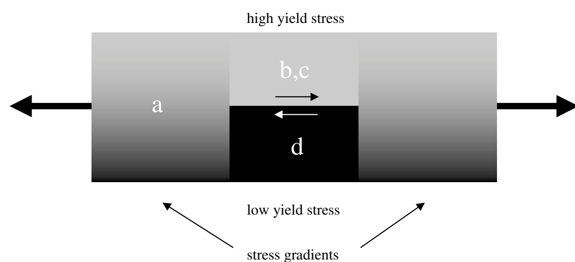

FIG. 2. Schematic of the scenario seen in thin film. Two grains of different yield stresses lead to shear stresses at the grain boundary and gradients in their neighbors.

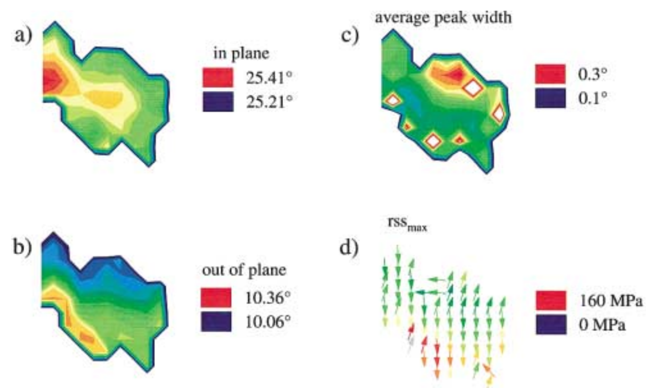

FIG. 3 (color). Single grain analysis: (a) in-plane orientation: angle between the (100) vector and the X axis, (b) out-of-plane orientation: angle between surface normal and the (111) direction, (c) average peak width, (d) vector plot of projection of glide directions experiencing the highest resolved shear stress; the color code corresponds to magnitude.

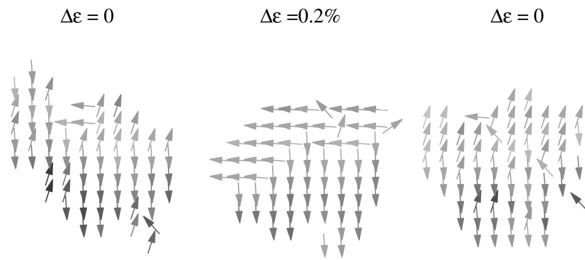

FIG. 4. Evolution of maximum resolved shear stress as a function of macroscopic strain in a bulge test (same grain as in Fig. 2) up to 0.2% total strain; vector plots of the projection of glide directions experiencing the highest resolved shear stress. Grey level corresponds to magnitude (white: 0 MPa; black: 140 MPa).

However, the division of the grain into two regimes has become more obvious.

Our results of probing thin film plasticity with submicron (and sub-grain-size) resolution reveal new aspects of deformation that have not previously been addressed in macroscopic thin film models [16–19]. Interactions between neighboring grains lead to highly nonuniform stresses in an individual grain and have led us to identify an effective grain size that is often much smaller than the physical size of a single grain. The surprising finding in this work is that grains that are much bigger than the film thickness, which would be expected to deform homogeneously, actually deform in a highly inhomogeneous fashion. This discovery can account for the wide distribution of yield stresses which in turn provides a basis for understanding macroscopic phenomena such as the Bauschinger effect. We anticipate that micro-Laue diffraction measurements of this kind will provide an understanding of the development of the room temperature stress distribution as it is established during cooldown from high temperature and will answer plasticity questions in even more complex materials with greater anisotropy, viz., copper. In general one can expect microdiffraction to have a strong impact on the measurement of 3D microcrystalline structures [20] as well as bulk polycrystalline samples [3], where local stress measurement is the key.

This research is supported by the Director, Office of Science, Office of Basic Energy Sciences, U.S. Department of Energy, under Contract No. DE-AC05-00OR22725 with UT-Battelle, LLC and with the Advanced Light Source, Materials Science Division, under Contract No. DE-AC03-76SF00098 at Lawrence Berkeley National Laboratory.

*Present address: Max-Planck-Institute for Metals Research, Stuttgart, Germany.
Electronic address: spolenak@mf.mpg.de

[1] F. Delaire, J. L. Raphanel, and C. Rey, Acta Mater. **48**, 1075–1087 (2000).
[2] D. Raabe, M. Sachtleber, Z. Zhao, F. Roters, and S. Zaefferer, Acta Mater. **49**, 3433–3441 (2001).
[3] L. Margulies, G. Winther, and H. F. Poulsen, Science **291**, 2392 (2001).
[4] D. P. Mika and P. R. Dawson, Mater. Sci. Eng. A **257**, 62 (1998).
[5] R.-M. Keller, S. P. Baker, and E. Arzt, J. Mater. Res. **13**, 1307–1317 (1998).
[6] J. S. Chung, N. Tamura, G. E. Ice, B. C. Larson, J. D. Budai, and W. Lowe, in *Materials Reliability in Microelectronics IX*, edited by C. A. Volkert, A. H. Verbruggen, and D. Brown, MRS Symposia Proceedings No. 563 (Materials Research Society, Pittsburgh, 1999), pp. 169–174.
[7] N. Tamura, J.-S. Chung, G. E. Ice, B. C. Larson, J. D. Budai, J. Z. Tischler, M. Yoon, E. L. Williams, and W. P. Lowe, in *Materials Reliability in Microelectronics IX*, (Ref. [6]), pp. 175–180.
[8] B. C. Larson, N. Tamura, J.-S. Chung, G. E. Ice, J. D. Budai, J. Z. Tischler, W. Yang, H. Weiland, and W. P. Lowe, Mater. Res. Soc. Symp. Proc. **590**, 247–252 (2000).
[9] N. Tamura, B. C. Valek, R. Spolenak, A. A. MacDowell, R. S. Celestre, H. A. Padmore, W. L. Brown, T. Marieb, J. C. Bravman, B.W. Batterman and J. R. Patel, Mater. Res. Soc. Symp. Proc. **612**, D8.8 (2000).
[10] A. A. MacDowell, R. S. Celestre, N. Tamura, R. Spolenak, B. Valek, W. L. Brown, J. C. Bravman, H. A. Padmore, B.W. Batterman, and J. R. Patel, Nucl. Instrum. Methods Phys. Res., Sect. A **467–468**, 936–943 (2001).
[11] N. Tamura, A. A. MacDowell, R. S. Celestre, H. A. Padmore, B. Valek, J. C. Bravman, R. Spolenak, W. L. Brown, T. Marieb, H. Fujimoto, B.W. Batterman, and J. R. Patel, Appl. Phys. Lett. **80**, 3724 (2002).
[12] J. S. Chung and G. E. Ice, J. Appl. Phys. **86**, 5249 (1999).
[13] R. Spolenak, D. L. Barr, M. E. Gross, K. Evans-Lutherodt, W. L. Brown, N. Tamura, A. A. MacDowell, R. S. Celestre, H. A. Padmore, J. R. Patel, B. C. Valek, J. C. Bravman, P. Flinn, T. Marieb, R. R. Keller, and B.W. Batterman, Mater. Res. Soc. Symp. Proc. **612,** D10.3 (2000).
[14] R. Spolenak, N. Tamura, B. C. Valek, D. L. Barr, M. D. Morris, J. F. Miner, W. L. Brown, A. A. MacDowell, R. S. Celestre, H. A. Padmore, J. C. Bravman, B.W. Batterman, and J. R. Patel, in *Proceedings of the Sixth International Workshop on Stress Related Phenomena in Metallization*, AIP Conf. Proc. No. 612, (AIP, Ithaca, NY, 2002), p. 217.
[15] R. Spolenak, C. A. Volkert, K. M. Takahashi, S. A. Fiorillo, J. F. Miner, and W. L. Brown, Mater. Res. Soc. Symp. Proc. **594**, 63–68 (1999).
[16] L. B. Freund, J. Appl. Mech. **54**, 553 (1987).
[17] W. D. Nix, Metall. Trans. A **20**, 2217 (1989).
[18] C.V. Thompson, J. Mater. Res. **8**, 237 (1993).
[19] J. E. Sanchez, Jr. and E. Arzt, Scr. Metall. Mater. **27**, 285–290 (1992).
[20] B. C. Larson, W. Yang, G. E. Ice, J. D. Budai, and J. Z. Tischler, Nature (London) **451**, 887 (2002).